HHS Public Access

Author manuscript

*Pediatr Radiol*. Author manuscript; available in PMC 2016 September 01.

Published in final edited form as:

*Pediatr Radiol*. 2015 September ; 45(10): 1431–1439. doi:10.1007/s00247-015-3336-6.

# Multidetector computed tomography pulmonary angiography in childhood acute pulmonary embolism

**Chun Xiang Tang**,
Department of Medical Imaging, Jinling Hospital, Medical School of Nanjing University, Nanjing, Jiangsu 210002, China

**U. Joseph Schoepf**,
Department of Medical Imaging, Jinling Hospital, Medical School of Nanjing University, Nanjing, Jiangsu 210002, China. Department of Radiology and Radiological Science, Medical University of South Carolina, Charleston, SC, USA. Department of Pediatrics, Medical University of South Carolina, Charleston, SC, USA

**Shahryar M. Chowdhury**,
Department of Pediatrics, Medical University of South Carolina, Charleston, SC, USA

**Mary A. Fox**,
Department of Radiology and Radiological Science, Medical University of South Carolina, Charleston, SC, USA

**Long Jiang Zhang**, and
Department of Medical Imaging, Jinling Hospital, Medical School of Nanjing University, Nanjing, Jiangsu 210002, China

**Guang Ming Lu**
Department of Medical Imaging, Jinling Hospital, Medical School of Nanjing University, Nanjing, Jiangsu 210002, China

Long Jiang Zhang: kevinzhlj@163.com

## Abstract

Pulmonary embolism is a life-threatening condition affecting people of all ages. Multidetector row CT pulmonary angiography has improved the imaging of pulmonary embolism in both adults and children and is now regarded as the routine modality for detection of pulmonary embolism. Advanced CT pulmonary angiography techniques developed in recent years, such as dual-energy CT, have been applied as a one-stop modality for pulmonary embolism diagnosis in children, as they can simultaneously provide anatomical and functional information. We discuss CT pulmonary angiography techniques, common and uncommon findings of pulmonary embolism in both conventional and dual-energy CT pulmonary angiography, and radiation dose considerations.

Correspondence to: Long Jiang Zhang, kevinzhlj@163.com.

**Conflicts of interest** None

**Keywords**

Acute pulmonary embolism; Children; CT pulmonary arteriography; Prognosis; Radiation dose

## Introduction

Pulmonary embolism is a potentially fatal disease and constitutes an important proportion of morbidity and mortality in adults [1, 2]. It is traditionally believed that the incidence of pulmonary embolism is much lower in children than in adults. However, recent studies using CT pulmonary angiography have demonstrated a high incidence (14–15.5%) of pulmonary embolism in children when there is clinical suspicion of such disease [3, 4]. In children with nephrotic syndrome, the frequency of pulmonary embolism was reported to be up to 17% [5]. This suggests that the frequency may previously have been underestimated in times when the diagnosis primarily relied on nonspecific clinical symptoms and laboratory data.

Imaging plays a vital role in evaluating pulmonary embolism. Historically, lung ventilation/perfusion scintigraphy was the primary diagnostic modality used in adults and children [6]. However, image interpretation difficulties and ventilation/perfusion mismatches due to confounding underlying disease processes are often encountered, thus lowering its specificity to detect pulmonary embolism [7]. With the rapid and substantial advancement of CT hardware and software, CT pulmonary angiography is now the primary imaging modality for evaluation of pulmonary embolism in adults and children due to its high sensitivity and specificity despite its disadvantages, such as iodinated contrast-induced nephropathy, radiation exposure and inability to provide lung functional (perfusion/ventilation) information [3, 7–11]. In recent years, dual-energy CT has been developed to detect pulmonary embolism in adults with the advantage of providing both anatomical and functional information in a single contrast-enhanced CT scan. This technique uses distinct X-ray spectra to visualize absorption characteristics of different types of materials and extracts maps of iodinated contrast material content using dedicated commercial software. The use of dual–energy CT for pulmonary embolism detection is increasing and has resulted in better recognition of the disease [7]. However, it is not yet standard practice for pulmonary embolism imaging in children. This review aims to discuss state-of-the-art CT pulmonary angiography techniques, CT pulmonary angiography findings of pulmonary embolism and radiation dose considerations in children.

## CT pulmonary angiography techniques

### CT scan techniques

Preparation before a CT pulmonary angiography scan is essential in children. Generally, children >5 years old can receive CT pulmonary angiography studies without sedation. Infants or children ≤5 years old should be sedated. If children ≤5 years old can follow the breathing instructions, CT pulmonary angiography may be attempted without sedation under the careful supervision of sedation nurses and CT technologists. If necessary, short-term sedation can be achieved, e.g., intravenous ketamine (1 mg/kg) has been reported [12].

However, duration of sedation can have an impact on pulmonary embolism evaluation due to development of dependent atelectasis.

Multidetector row computed tomography scanning protocols in children depend on CT hardware and patient age. Table 1 gives dual-source and single-source CT pulmonary angiography scanning parameters in children based on our experience. CT pulmonary angiography is performed supine with scanning direction from cranial to caudal, from the lung apices to the diaphragm. In infants and younger children, CT examinations are performed at resting lung volumes. For children following breathing instructions, full inspiration breath-holding should be avoided to reduce its adverse effect on pulmonary arterial enhancement [13].

Dual-energy CT has been used to detect pulmonary embolism in children. The various technical implementations of this approach, such as dual-source CT, rapid kilovoltage switching and sandwich detector approaches are beyond the scope of this review. The technical foundations of dual-energy CT applications have been reviewed elsewhere [14–16]. Of the above-mentioned dual-energy CT techniques, dual-source CT and rapid kilovoltage switching, especially the former, have broad clinical application in pulmonary embolism evaluation. Herein, we provide recommendations for image acquisition parameters using these two dual-energy CT techniques for pulmonary embolism evaluation in children.

Recommended contrast medium injection protocols for pediatric CT pulmonary angiography are listed in Table 2. Bolus tracking method is recommended to obtain the optimal delay time for CT pulmonary angiography; the scan should be initiated 4 s after pulmonary artery trunk enhancement is greater than 100 Hounsfield units. As with all CT imaging, achieving a radiation dose as low as reasonably possible (ALARA principle) should always be the goal when performing CT pulmonary angiography in the evaluation of children with suspected pulmonary embolism.

## Iodinated contrast media injection techniques

Before intravenously injecting contrast media, clinical information should be obtained, such as history of prior reaction to iodinated contrast media, history of severe allergies, history of renal insufficiency and current use of metformin-containing medication [12]. Maximal contrast media injection rates for children should be adjusted according to the cannula size as follows: 5.0 mL/s for 16- to 18-gauge cannula, 4.0 mL/s for 20-gauge cannula, 2.5 mL/s for 22-gauge cannula. A rate of 1.0 mL/s is acceptable for very small patients (<15 kg) using a 24-gauge cannula, often by hand injection. When peripheral venous access is not possible, central venous catheters can be used for injection of contrast media, and implanted ports and peripherally inserted central catheters specifically designed for use with power injectors are suggested. Detailed iodinated contrast media injection parameters can be found in Table 2 [14, 17–19].

## Post-processing techniques

Multiplanar reformatted CT images in the coronal and sagittal planes can be created using standard reconstruction algorithms. Multiplanar reformatted images are more sensitive in detecting superior pulmonary artery emboli compared with axial enhanced CT images. Lee et al. [20] assessed the use of multiplanar reformatted CT images in the pulmonary embolism diagnosis in 60 children and found that its use significantly increased diagnostic confidence and interobserver agreement; however, image interpretation time was increased for radiology residents. They concluded that multiplanar reformatted images should be integrated into routine practice. Slab reformatting with maximum intensity projection and clinical software applications, such as computer-aided diagnosis, dual-energy CT based lung perfusion imaging, and rendering of lung vessels from dual-energy CT data sets, are used to help establish the diagnosis both in adults and children [21, 22]. Although these advanced reformatted images can help detect pulmonary emboli, axial thin-section CT images are the mainstay for pulmonary embolism evaluation in children because these axial enhanced images not only exhibit the lung parenchyma and pulmonary vessel changes seen with pulmonary embolism but also present cardiac morphological information.

## CT findings of acute pulmonary embolism

Findings of pulmonary embolism on CT imaging can be classified into four categories: pulmonary artery findings, pulmonary parenchyma, lung function and cardiac abnormalities. Other indirect findings, such as pleural effusion, can also be used to help identify pulmonary embolism in children.

### Pulmonary artery manifestations

Pulmonary emboli in the proximal vessels have similar findings in adults and children. Contrast-enhanced axial or reformatted CT images show complete occlusion of one or both of the pulmonary arteries (Fig. 1), an eccentric partial filling defect (Fig. 2), a central partial filling defect (Fig. 2) or a combination of the above. The affected artery is frequently dilated compared to the opposite side [23] (Fig. 1). Kritsaneepaiboon et al. [4] found a lower lobe predilection (right lower lung lobe>left lower lung lobe) of pulmonary embolism in children, as seen in adults. Thus, detailed assessment of pulmonary arteries in both lower lung lobes should be emphasized in routine clinical practice.

Studies have shown a high diagnostic performance of multidetector CT pulmonary angiography for pulmonary embolism detection in children [3, 4]. Compared with central pulmonary emboli, identification of peripheral (subsegmental) pulmonary embolism in children is more difficult due to the small size of pulmonary vessels of children. Even in adults, several studies have reported that small peripheral emboli have a high risk of remaining unidentified [24–26]. Ritchie et al. [2] reported that more than 30% of peripheral pulmonary emboli may be missed on initial review. Multiple techniques can be used to improve diagnostic accuracy of CT pulmonary angiography. For example, the use of multiplanar reformatted images significantly improves image interpretation among radiologists for diagnosing pulmonary embolism in children.

While some of the newest methods for improving diagnostic accuracy of CT pulmonary angiography have not yet been studied in children, multiple techniques studied in adults have the potential to be used in children and merit further study. For example, computerized algorithms can alleviate perceptual error and thus have the potential to facilitate peripheral pulmonary embolism diagnosis [27]. The rate of missed pulmonary emboli on CT can be reduced by the use of these computer-assisted diagnosis systems that have been developed to aid radiologists in the recognition of endovascular clots. Used as a second reader, computer-assisted diagnosis can help detect small emboli initially missed [28, 29], increasing reader sensitivity in diagnosis of peripheral pulmonary embolism. In addition, the high negative predictive value of these tools is helpful in reassuring inexperienced readers [30].

Kligerman et al. [31] reviewed those studies with false-negative results for pulmonary embolism in prior CT pulmonary angiography studies in 6,769 patients by using the computer-assisted diagnosis system. They found that the computer-assisted diagnosis system identified at least one pulmonary embolus in 77.4% of CT pulmonary angiography studies with an initial false-negative interpretation. Limitations of computer-assisted diagnosis, such as a small increase in interpretation time and an increase in false-positive findings, should be recognized when utilizing this system in clinical practice [32].

Another method to improve peripheral pulmonary embolism detection is use of a software algorithm that can evaluate intravascular iodine distribution in dual-energy CT angiography. The software is applied to highlight iodine distribution in small pulmonary vessels, especially in peripheral pulmonary vessels. Images with high iodine content are color-coded blue and soft tissue or vessels with low or no iodine content due to pulmonary embolism are color-coded red; indeterminate iodine concentrations are color-coded gray (Fig. 3) [33]. Clinical studies have demonstrated the potential of vascular iodine distribution detection in improving peripheral pulmonary embolism detection [5, 33, 34]. In addition, Tang et al. [35] demonstrated the advantages of such software in the detection of small peripheral clots with an animal model. They found that use of vascular iodine distribution software can significantly improve the sensitivity of detecting subsegmental pulmonary embolism compared with conventional CT pulmonary angiography, using pathological specimens as the gold standard.

## Pleural and pulmonary parenchymal abnormalities

Lung and pleural abnormalities can indicate pulmonary embolism diagnosis and improve pulmonary embolism detection in children. Westermark’s sign is defined as oligemic segments of the lung affected by the emboli. Oligemia, or a decreased blood flow rate, is characterized by a mosaic pattern on lung window CT images. A large acute central pulmonary embolus can cause oligemia of the corresponding lung and dilation in vessel diameter (Fig. 1). Hampton’s hump is a peripheral wedge-shaped consolidation with the peak directed to the pulmonary hilum (Fig. 4). Its presence on CT pulmonary angiography is associated with pulmonary embolism in children [36]. Other signs, such as atelectasis and ipsilateral pleural effusion, are also associated with pulmonary embolism in children (Fig. 4).

## Functional abnormalities

Regional lung perfusion and ventilation function can be evaluated with dual-energy CT, which provides both high-resolution anatomical information and functional details in one contrast-enhanced CT exam. These techniques have shown promise when used in children with suspected pulmonary embolism [14, 16, 34, 37]. In fact, detection of pulmonary embolism is the most common indication of dual-energy CT lung perfusion imaging. This technique may provide additional clinical information over that obtained by CT pulmonary angiography alone as it can detect the degree and significance of the affected lung tissue downstream of the pulmonary embolism [38]. It has been observed that the ratio of low and high kilovoltage CT-values relative to air is only a reflection of iodine within lung vessels [39]. Therefore, dual-energy CT lung perfusion imaging relies on the difference of the slope ratio between the lung vessels filled with and without iodine. Dual-energy CT lung perfusion images are generated on a single acquisition and thus represent the static iodine distribution in the pulmonary capillary circulation at a single time point. In dual-energy CT lung perfusion imaging, wedge-shaped or triangular-shaped defects are known to be suggestive of acute pulmonary embolism. Zhang et al. [40] confirmed that dual-energy CT evidence of abnormal pulmonary perfusion improved the detection of acute pulmonary embolism in a rabbit model, particularly emphasizing the presence of subsegmental wedge-shaped lung perfusion defects. Others [33, 34, 41, 42] have shown that dual-energy CT lung perfusion imaging provides additional diagnostic value to detect non-obstructive pulmonary emboli and subsegmental perfusion defects without identifiable pulmonary emboli compared with CT pulmonary angiography alone in children and adults (Fig. 3).

In dual-energy CT lung perfusion images, artifacts that may be mistaken as perfusion defects are important to recognize to avoid false-positive results. Gravity-dependent lung perfusion in lung perfusion images obtained in the supine position appear as low perfusion (color-coded blue) in relative ventral side and high perfusion (color-coded red or yellow) in relative dorsal side. Beam-hardening artifacts due to high-attenuation iodinated contrast media in the systemic veins can cause the appearance of radial perfusion abnormalities adjacent to the systemic veins. Respiratory and cardiac pulsation artifacts are often encountered in dual-energy CT lung perfusion images. These artifacts are characterized by their linear appearance in coronal and sagittal plane lung perfusion images as opposed to the wedge-shaped defects in true pulmonary embolism (Fig. 5) [40].

## Cardiac manifestations

Cardiac abnormalities of acute pulmonary embolism in CT pulmonary angiography include right ventricular dilatation, interventricular septal bowing into the left ventricle, inferior vena cava, superior vena cava and azygous vein dilatation, and contrast media reflux into the inferior vena cava. The right ventricular/left ventricular diameter ratio is one of the most important parameters to evaluate as it has been linked to the hemodynamic severity of pulmonary embolism, inhospital morbidity and mortality, and adverse clinical events such as early death [43, 44]. Several practical approaches have been proposed to determine the right ventricular/left ventricular diameter ratio, including measurements on axial CT sections, short-axis images and 4-chamber views of the cardiac cavities. A right ventricular/left ventricular diameter ratio >1 in transverse images or right ventricular/left ventricular

diameter ratio >0.9 in 4-chamber images is regarded as having right heart dysfunction in adults (Fig. 6). One recent meta-analysis revealed an association between right ventricular/left ventricular diameter ratio and mortality in patients with pulmonary embolism [45]. However, no data have yet been reported in children with pulmonary embolism.

### Evaluating the severity of pulmonary embolism in children

Prognostic models that accurately risk-stratify this population have been developed in adults. Adult patients classified as low risk by these models can be safely treated as outpatients [46]. Evaluating the prognosis of pulmonary embolism in children using CT pulmonary angiography has been sparsely studied. The CT pulmonary angiography prognostic parameters found in adults [47, 48] have the potential to be used as important tools when assessing the prognostic utility of CT pulmonary angiography in children.

Pulmonary artery obstruction indices for evaluating the severity of pulmonary embolism also merit further study in children, including the Miller index, Walsh index, Qanadli index and Mastora index. Reports evaluating the pulmonary artery obstruction indices' association with mortality have been mixed [49, 50]. A recent meta-analysis showed the location of pulmonary artery obstruction of patients with acute pulmonary embolism on CT pulmonary angiography can be used for risk stratification; however, there was no correlation between these indexes and prognosis [51].

Perfusion defect scoring has been used to evaluate pulmonary embolism severity in adults and has potential in children. Two perfusion defect scoring algorithms have been well studied, the semiquantitative pulmonary perfusion defect score and the quantitative perfusion defect volume. Bauer et al. [52] and Apfaltrer et al. [53] also found a dual-energy CT-based perfusion defect score correlated with pulmonary embolism severity.

## Radiation dose consideration

In recent years, ionizing radiation derived from CT has attracted more and more attention, especially for children, because of their vulnerability to ionizing radiation compared to adults [54, 55]. Recent studies reported radiation doses of children undergoing CT pulmonary angiography ranged from 2 to 26 mSv. Importantly, there is no added radiation dose with dual-energy CT compared to CT pulmonary angiography [4, 12, 34, 56]. For example, Zhang et al. [34] reported the mean effective radiation dose from dual-energy CT pulmonary angiography was 2.3±1.1 mSv (range: 1.1 to 7.1 mSv) in 32 children with nephrotic syndrome, which was comparable to or lower than effective dose reported in previous studies using single-source, single-energy CT pulmonary angiography. Victoria et al. [3] reported that the mean effective dose was 2–5 mSv, while Kritsaneepaiboon et al. [4] reported mean effective dose as 10.5 mSv (range: 2.3–26 mSv). The range of radiation doses in children undergoing CT pulmonary angiography stems from the varying CT equipment and the scanning parameters at different centers. Thus, it is important to standardize scanning protocols aimed at radiation dose reduction for CT pulmonary angiography in children.

Reduced radiation dose can be achieved by two methods. One is the strict control of indications for CT pulmonary angiography to reduce overutilization in the population. Another is individual radiation dose reduction. With the attractiveness of the utilization of CT pulmonary angiography in children with suspected pulmonary embolism, the concern of potential overutilization of CT pulmonary angiography is increasing. Lee et al. [18] suggested that with the use of risk factor assessment, CT pulmonary angiography can be used more appropriately to substantially reduce costs and radiation exposure in children with clinically suspected pulmonary embolism. Overall, improved understanding of the recommended guidelines, evidence-based literature, and current concepts in assessment of pulmonary embolism by both radiologists and clinicians will reduce unnecessary CT pulmonary angiography examinations.

Many radiation-saving techniques can be used in pediatric CT pulmonary angiography studies: lower tube current, automatic tube current modulation, lower tube voltage, automatic tube voltage modulation, shortening scan time (high-pitch) or a combination of these methods. These techniques can substantially reduce radiation dose compared with standard CT pulmonary angiography techniques. Importantly, iterative reconstruction is recommended to improve image quality when dose saving techniques are used. In addition, the use of low tube voltage or high-pitch technique has the potential to reduce iodinated contrast agent volume by increasing iodine contrast noise ratio or shortening scan time while maintaining diagnostic image quality [57, 58].

## Conclusion

Pulmonary embolism is a life-threatening disease in children and diagnosis has important implications for clinical care and outcomes. State-of-the-art CT pulmonary angiography can evaluate the pulmonary arteries, pulmonary parenchyma, some pathophysiological parameters and the heart, and hence has prognostic potential. The amount of ionizing radiation in pediatric application should be carefully monitored and minimized.

## Acknowledgments

This work was partially supported by the Program for New Century Excellent Talents in the University (NCET-12-0260) and Natural Science Foundation of China (No. 81401409 for C.X.T.).

## References

1. Tapson VF. Acute pulmonary embolism. N Engl J Med. 2008; 358:1037–1052. [PubMed: 18322285]
2. Ritchie G, McGurk S, McCreath C, et al. Prospective evaluation of unsuspected pulmonary embolism on contrast enhanced multidetector CT (MDCT) scanning. Thorax. 2007; 62:536–540. [PubMed: 17158631]
3. Victoria T, Mong A, Altes T, et al. Evaluation of pulmonary embolism in a pediatric population with high clinical suspicion. Pediatr Radiol. 2009; 39:35–41. [PubMed: 19005649]
4. Kritsaneepaiboon S, Lee EY, Zurakowski D, et al. MDCT pulmonary angiography evaluation of pulmonary embolism in children. AJR Am J Roentgenol. 2009; 192:1246–1252. [PubMed: 19380547]

5. Zhang LJ, Zhang Z, Li SJ, et al. Pulmonary embolism and renal vein thrombosis in patients with nephrotic syndrome: prospective evaluation of prevalence and risk factors with CT. Radiology. 2014; 273:897–906. [PubMed: 25072187]
6. Rajpurkar M, Warrier I, Chitlur M, et al. Pulmonary embolism—experience at a single children's hospital. Thromb Res. 2007; 119:699–703. [PubMed: 16879861]
7. Babyn PS, Gahunia HK, Massicotte P. Pulmonary thrombo-embolism in children. Pediatr Radiol. 2005; 35:258–274. [PubMed: 15635472]
8. Henzler T, Barraza JM Jr, Nance JW Jr, et al. CT imaging of acute pulmonary embolism. J Cardiovasc Comput Tomogr. 2011; 5:3–11. [PubMed: 21051309]
9. Sanchez O, Planquette B, Meyer G. Update on acute pulmonary embolism. Eur Respir Rev. 2009; 18:137–147. [PubMed: 20956134]
10. Stein PD, Fowler SE, Goodman LR, et al. Multidetector computed tomography for acute pulmonary embolism. N Engl J Med. 2006; 354:2317–2327. [PubMed: 16738268]
11. Lee EY, Zurakowski D, Boiselle PM. Pulmonary embolism in pediatric patients: survey of CT pulmonary angiography practices and policies. Acad Radiol. 2010; 17:1543–1549. [PubMed: 20934355]
12. Yu FF, Lu B, Gao Y, et al. Congenital anomalies of coronary arteries in complex congenital heart disease: diagnosis and analysis with dual-source CT. J Cardiovasc Comput Tomogr. 2013; 7:383–390. [PubMed: 24331934]
13. Li YJ, Lau KK, Ardley N, et al. Efficacy of 'breath holding at ease' during CT pulmonary angiography in the improvement of contrast enhancement in pulmonary arteries. J Med Imaging Radiat Oncol. 2013; 57:415–422. [PubMed: 23870336]
14. Goo HW. Dual-energy lung perfusion and ventilation CT in children. Pediatr Radiol. 2013; 43:298–307. [PubMed: 23417255]
15. Lu GM, Zhao Y, Zhang LJ, et al. Dual-energy CT of the lung. AJR Am J Roentgenol. 2012; 199:S40–S53. [PubMed: 23097167]
16. Ko JP, Brandman S, Stember J, et al. Dual-energy computed tomography: concepts, performance, and thoracic applications. J Thorac Imaging. 2012; 27:7–22. [PubMed: 22189245]
17. Callahan MJ, Servaes S, Lee EY, et al. Practice patterns for the use of iodinated IV contrast media for pediatric CT studies: a survey of the Society for Pediatric Radiology. AJR Am J Roentgenol. 2014; 202:872–879. [PubMed: 24660719]
18. Lee EY, Tse SK, Zurakowski D, et al. Children suspected of having pulmonary embolism: multidetector CT pulmonary angiography–thromboembolic risk factors and implications for appropriate use. Radiology. 2012; 262:242–251. [PubMed: 22106353]
19. Lee EY, Neuman MI, Lee NJ, et al. Pulmonary embolism detected by pulmonary MDCT angiography in older children and young adults: risk factor assessment. AJR Am J Roentgenol. 2012; 198:1431–1437. [PubMed: 22623559]
20. Lee EY, Zucker EJ, Tsai J, et al. Pulmonary MDCT angiography: value of multiplanar reformatted images in detecting pulmonary embolism in children. AJR Am J Roentgenol. 2011; 197:1460–1465. [PubMed: 22109303]
21. Maizlin ZV, Vos PM, Godoy MC, et al. Computer-aided detection of pulmonary embolism on CT angiography: initial experience. J Thorac Imaging. 2007; 22:324–329. [PubMed: 18043386]
22. Buhmann S, Herzog P, Liang J, et al. Clinical evaluation of a computer-aided diagnosis (CAD) prototype for the detection of pulmonary embolism. Acad Radiol. 2007; 14:651–658. [PubMed: 17502254]
23. Wittram C, Kalra MK, Maher MM, et al. Acute and chronic pulmonary emboli: angiography-CT correlation. AJR Am J Roentgenol. 2006; 186:S421–S429. [PubMed: 16714619]
24. Brunot S, Corneloup O, Latrabe V, et al. Reproducibility of multidetector spiral computed tomography in detection of sub-segmental acute pulmonary embolism. Eur Radiol. 2005; 15:2057–2063. [PubMed: 16021452]
25. Le Gal G, Righini M, Parent F, et al. Diagnosis and management of subsegmental pulmonary embolism. J Thromb Haemost. 2006; 4:724–731. [PubMed: 16634736]

26. Ghanima W, Nielssen BE, Holmen LO, et al. Multidetector computed tomography (MDCT) in the diagnosis of pulmonary embolism: interobserver agreement among radiologists with varied levels of experience. Acta Radiol. 2007; 48:165–170. [PubMed: 17354136]
27. Schoepf UJ, Schneider AC, Das M, et al. Pulmonary embolism: computer-aided detection at multidetector row spiral computed tomography. J Thorac Imaging. 2007; 22:319–323. [PubMed: 18043385]
28. Wittenberg R, Peters JF, Sonnemans JJ, et al. Computer-assisted detection of pulmonary embolism: evaluation of pulmonary CT angiograms performed in an on-call setting. Eur Radiol. 2010; 20:801–806. [PubMed: 19862534]
29. Lee CW, Seo JB, Song JW, et al. Evaluation of computer-aided detection and dual-energy software in detection of peripheral pulmonary embolism on dual-energy pulmonary CT angiography. Eur Radiol. 2011; 21:54–62. [PubMed: 20680290]
30. Blackmon KN, Florin C, Bogoni L, et al. Computer aided detection of pulmonary embolism at CT pulmonary angiography: can it improve performance of inexperienced readers? Eur Radiol. 2011; 21:1214–1223. [PubMed: 21225269]
31. Kligerman SJ, Lahiji K, Galvin JR, et al. Missed pulmonary emboli on CT angiography: assessment with pulmonary embolism-computer-aided detection. AJR Am J Roentgenol. 2014; 202:65–73. [PubMed: 24370130]
32. Wittenberg R, Berger FH, Peters JF, et al. Acute pulmonary embolism: effect of a computer assisted detection prototype on diagnosis—an observer study. Radiology. 2012; 262:305–313. [PubMed: 22190659]
33. Krissak R, Henzler T, Reichert M, et al. Enhanced visualization of lung vessels for diagnosis of pulmonary embolism using dual energy CT angiography. Invest Radiol. 2010; 45:341–346. [PubMed: 20421798]
34. Zhang LJ, Wang ZJ, Zhou CS, et al. Evaluation of pulmonary embolism in pediatric patients with nephrotic syndrome with dual energy CT pulmonary angiography. Acad Radiol. 2012; 19:341–348. [PubMed: 22177283]
35. Tang CX, Zhang LJ, Han ZH, et al. Dual-energy CT based vascular iodine analysis improves sensitivity for peripheral pulmonary artery thrombus detection: an experimental study in canines. Eur J Radiol. 2013; 82:2270–2278. [PubMed: 23891532]
36. Lee EY, Zurakowski D, Diperna S, et al. Parenchymal and pleural abnormalities in children with and without pulmonary embolism at MDCT pulmonary angiography. Pediatr Radiol. 2010; 40:173–181. [PubMed: 19847415]
37. Kang MJ, Park CM, Lee CH, et al. Dual-energy CT: clinical applications in various pulmonary diseases. Radiographics. 2010; 30:685–698. [PubMed: 20462988]
38. Wildberger JE, Schoepf UJ, Mahnken AH, et al. Approaches to CT perfusion imaging in pulmonary embolism. Semin Roentgenol. 2005; 40:64–73. [PubMed: 15732562]
39. Hansell DM, Bankier AA, MacMahon H, et al. Fleischner Society: glossary of terms for thoracic imaging. Radiology. 2008; 246:697–722. [PubMed: 18195376]
40. Zhang LJ, Zhao YE, Wu SY, et al. Pulmonary embolism detection with dual-energy CT: experimental study of dual-source CT in rabbits. Radiology. 2009; 252:61–70. [PubMed: 19561250]
41. Goo HW. Initial experience of dual-energy lung perfusion CT using a dual-source CT system in children. Pediatr Radiol. 2010; 40:1536–1544. [PubMed: 20596701]
42. Thieme SF, Johnson TR, Reiser MF, et al. Dual-energy lung perfusion CT: a novel pulmonary functional imaging method. Semin Ultrasound CT MR. 2010; 31:301–308. [PubMed: 20691930]
43. Ghuysen A, Ghaye B, Willems V, et al. Computed tomographic pulmonary angiography and prognostic significance in patients with acute pulmonary embolism. Thorax. 2005; 60:956–961. [PubMed: 16131526]
44. Ghaye B, Ghuysen A, Willems V, et al. Severe pulmonary embolism: pulmonary artery clot load scores and cardiovascular parameters as predictors of mortality. Radiology. 2006; 239:884–891. [PubMed: 16603659]
45. Becattini C, Agnelli G, Germini F, et al. Computed tomography to assess risk of death in acute pulmonary embolism: a meta-analysis. Eur Respir J. 2014; 43:1678–1690. [PubMed: 24603813]

46. Erkens PM, Gandara E, Wells PS, et al. Does the Pulmonary Embolism Severity Index accurately identify low risk patients eligible for outpatient treatment? Thromb Res. 2012; 129:710–714. [PubMed: 21906787]
47. Kang DK, Thilo C, Schoepf UJ, et al. CT signs of right ventricular dysfunction: prognostic role in acute pulmonary embolism. JACC Cardiovasc Imaging. 2011; 4:841–849. [PubMed: 21835376]
48. Kang DK, Ramos-Duran L, Schoepf UJ, et al. Reproducibility of CT signs of right ventricular dysfunction in acute pulmonary embolism. AJR Am J Roentgenol. 2010; 194:1500–1506. [PubMed: 20489089]
49. van der Meer RW, Pattynama PM, van Strijen MJ, et al. Right ventricular dysfunction and pulmonary obstruction index at helical CT: prediction of clinical outcome during 3-month follow-up in patients with acute pulmonary embolism. Radiology. 2005; 235:798–803. [PubMed: 15845793]
50. Nural MS, Elmali M, Findik S, et al. Computed tomographic pulmonary angiography in the assessment of severity of acute pulmonary embolism and right ventricular dysfunction. Acta Radiol. 2009; 50:629–637. [PubMed: 19488895]
51. Vedovati MC, Germini F, Agnelli G, et al. Prognostic role of embolic burden assessed at computed tomography angiography in patients with acute pulmonary embolism: systematic review and meta-analysis. J Thromb Haemost. 2013; 11:2092–2102. [PubMed: 24134450]
52. Bauer RW, Frellesen C, Renker M, et al. Dual energy CT pulmonary blood volume assessment in acute pulmonary embolism - correlation with D-dimer level, right heart strain and clinical outcome. Eur Radiol. 2011; 21:1914–1921. [PubMed: 21533631]
53. Apfaltrer P, Bachmann V, Meyer M, et al. Prognostic value of perfusion defect volume at dual energy CTA in patients with pulmonary embolism: correlation with CTA obstruction scores, CT parameters of right ventricular dysfunction and adverse clinical outcome. Eur J Radiol. 2012; 81:3592–3597. [PubMed: 22495202]
54. Mayo J, Thakur Y. Acute pulmonary embolism: from morphology to function. Semin Respir Crit Care Med. 2014; 35:41–49. [PubMed: 24481758]
55. Macdougall RD, Strauss KJ, Lee EY. Managing radiation dose from thoracic multidetector computed tomography in pediatric patients: background, current issues, and recommendations. Radiol Clin N Am. 2013; 51:743–760. [PubMed: 23830796]
56. Lee EY, Kritsaneepaiboon S, Zurakowski D, et al. Beyond the pulmonary arteries: alternative diagnoses in children with MDCT pulmonary angiography negative for pulmonary embolism. AJR Am J Roentgenol. 2009; 193:888–894. [PubMed: 19696306]
57. Li Q, Yu H, Zhang L, et al. Combining low tube voltage and iterative reconstruction for contrast-enhanced CT imaging of the chest-Initial clinical experience. Clin Radiol. 2013; 68:e249–e253. [PubMed: 23428340]
58. Lu GM, Luo S, Meinel FG, et al. High-pitch computed tomography pulmonary angiography with iterative reconstruction at 80 kVp and 20 mL contrast agent volume. Eur Radiol. 2014; 24:3260–3268. [PubMed: 25100336]

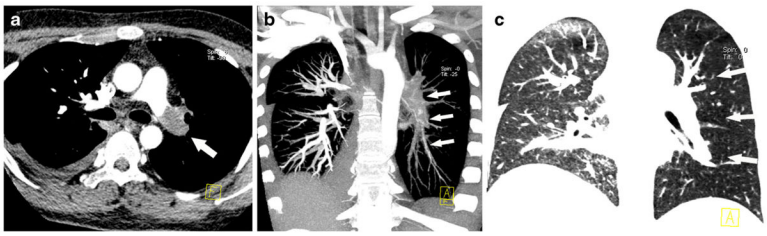


**Fig. 1.**

Complete occlusion of the left pulmonary artery in a 13-year-old boy with focal segmental glomerulosclerosis. **a** Contrast-enhanced axial CT image shows low-attenuation complete filling defect in left pulmonary artery and dilation of the artery (*arrow*). **b** Coronal maximum intensity projection image shows filling defect in left pulmonary arteries (*arrows*). **c** Coronal image with lung window shows the left lung oligemia caused by the large central pulmonary embolus (*arrows*)

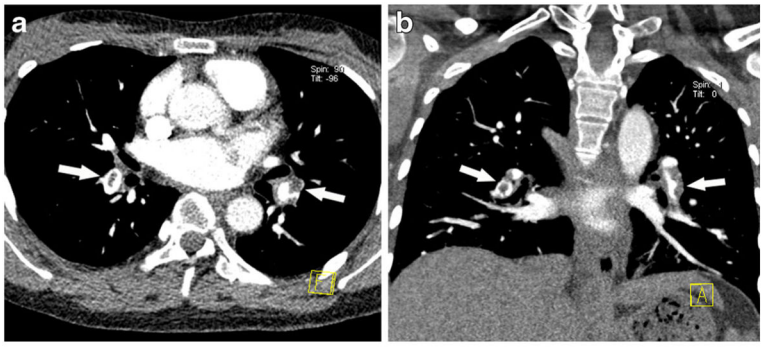


**Fig. 2.**

Partial filling defects of multiple pulmonary arteries in a 15-year-old girl with systemic lupus erythematosus. **a**–**b** Axial and coronal contrast-enhanced CT images demonstrate central filling defect in right pulmonary artery branch and eccentric partial filling defect in left pulmonary artery branch (*arrows*)

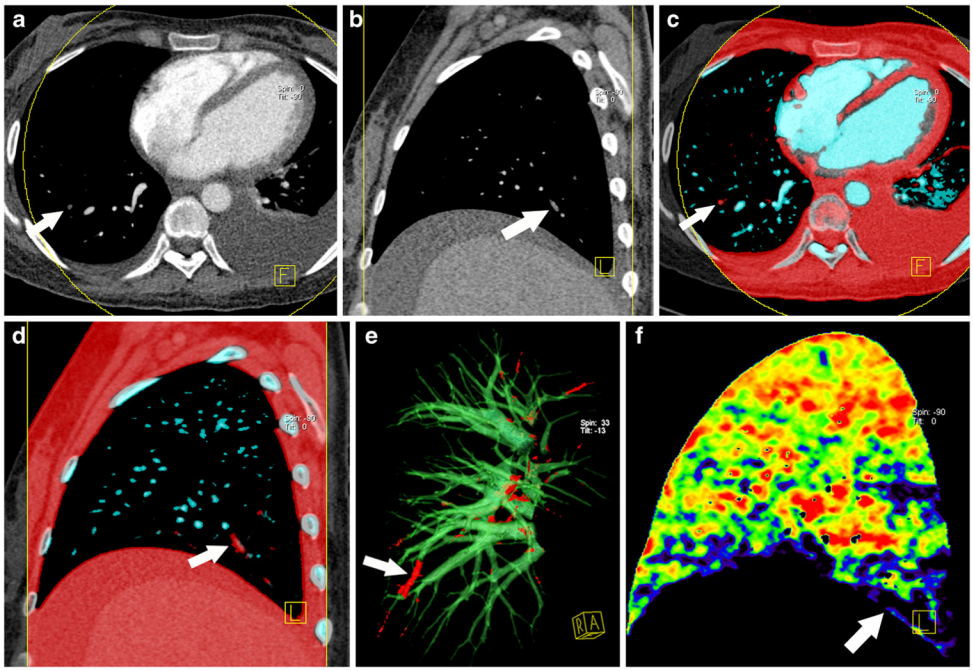


**Fig. 3.**

Dual-energy CT with vascular rendering in the detection of pulmonary embolus in a 14-year-old boy with podocytopathy. **a–b** Conventional CT images and (**c–f**) parametricized CT images from the same scan. Right lower pulmonary arteries are coded red (*arrows* in **c–e**) and the other pulmonary arteries are coded blue, which correspond to *arrows* in **a–b** in conventional CT pulmonary angiography. A perfusion defect is demonstrated with vascular rendering (*arrow* in **f**) in corresponding lung segment

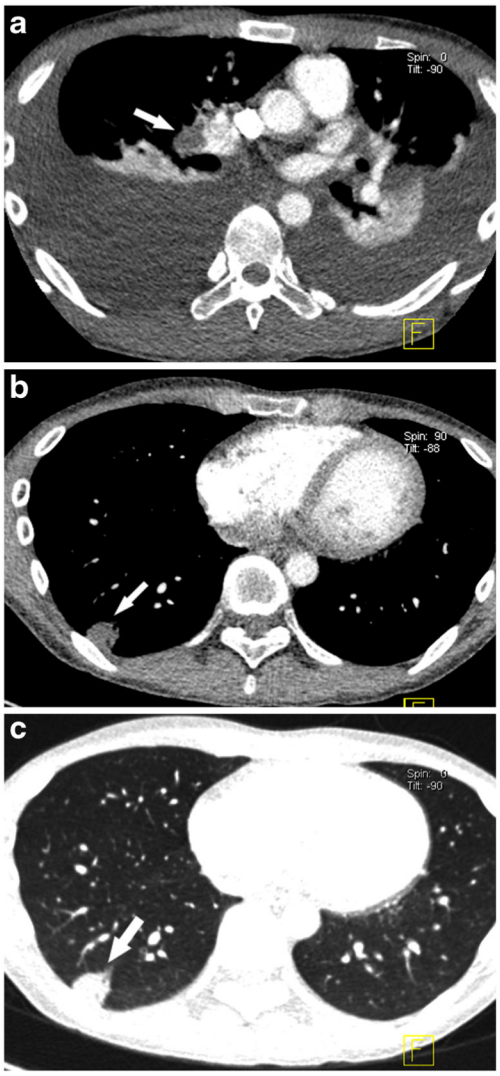


**Fig. 4.**

Hampton's hump in a 17-year-old girl with focal segmental glomerulosclerosis. **a** Axial contrast-enhanced CT image illustrates a pulmonary embolus (*arrow*) in the right pulmonary artery trunk and bilateral pleural effusion. **b–c** One month later, follow-up dual-energy CT images show a subpleural triangular lung infarct (Hampton's hump; *white arrows*)

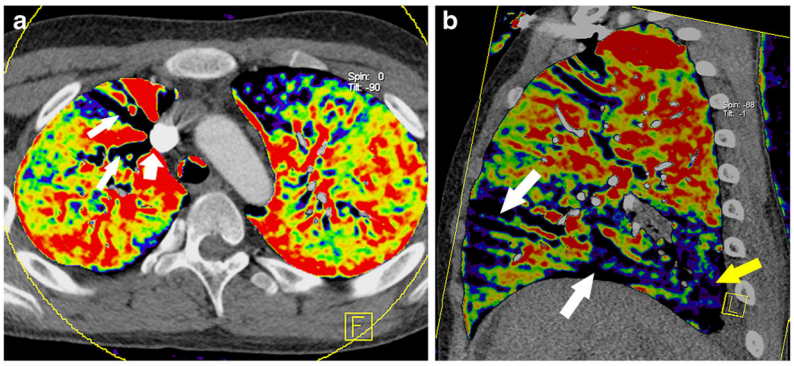


**Fig. 5.**

Common artifacts mimicking perfusion defects in dual-energy CT lung perfusion imaging in a 10-year-old boy with nephrotic syndrome. **a–b** Beam hardening artifacts and respiratory artifacts in dual-energy CT lung perfusion images. Radial beam hardening artifacts (*thin white arrows*) appear around vessels (*thick white arrow*) filled with contrast agent (**a**). Respiratory artifacts could be recognized in sagittal image as strip-shaped (*white arrows*) rather than wedge-shaped (*yellow arrow* in **b**)

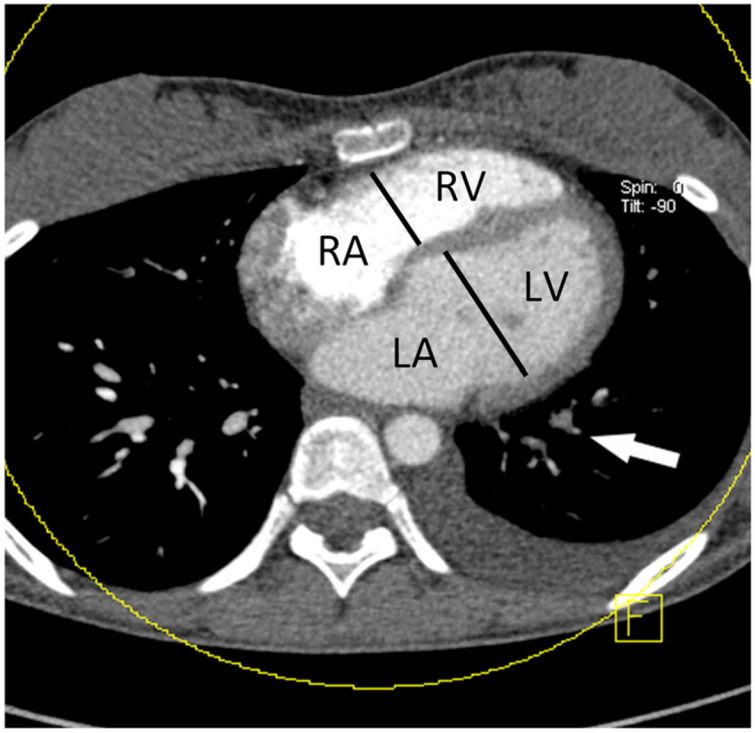


**Fig. 6.**

Maximal diameter measurement of the right and left ventricles in axial contrast-enhanced CT image in a 15-year-old girl with podocytopathy. Measurements should be performed at the levels of right and left atrioventricular valve. Note the filling defects in the left inferior pulmonary arteries (*arrow*). *RA* right atrium, *LA* left atrium, *RV* right ventricle, *LV* left ventricle

## Table 1

Recommended CT parameters for pediatric dual-energy CT pulmonary angiography

| Parameters | Dual-source CT | | Single-source CT |
|---|---|---|---|
| | First generation | Second generation | |
| Tube potential (kV) | 80/140 | 80/Sn140* | 80 |
| Effective tube current (mAs) | 213/50 | 89/38 | 100 |
| Tube current modulation | Yes | Yes | Yes |
| Collimation** | 64×0.6 | 128×0.6 | 64/128×0.6 |
| Pitch | 0.5 | 1.0 | 1.0–1.2 |
| Rotation time(s) | 0.33 | 0.28 | 0.5 |
| Pixel matrix | 512×512 | 512×512 | 512×512 |
| Section thickness (mm) | 0.75/0.5 | 0.75/0.5 | 0.75/0.5 |
| Energy ratio# | 0.3 | 0.3 | – |

*Sn indicates the tin plate that is used to filter high-energy rays of low energy components, that is selected photon shield (SPS) in second-generation dual-source CT

**with the z-flying focal spot technique

#energy ratio indicates a low- and high-kilovoltage linear weighting coefficient. Linear weighting coefficient of 0.3 denotes 30% image information from low-kilovoltage series and 70% from 140-kVp series

**Table 2**

Recommended contrast medium injection parameters for CT pulmonary angiography in children

| Contrast medium injection techniques | Recommended parameters |
|---|---|
| Contrast medium | Nonionic contrast medium |
| Dose of contrast medium | 1.0–1.5 ml/kg (or ≤60 ml) |
| Iodine concentration | 300 mg I/ml |
| Size of catheter | ≥22-G catheter for >5 years old, <22-G catheter for <5 years old |
| Methods of injection | High-pressure syringe for >5 years old, hand push for <5 years old |
| Injection rate | 1 ml/s for a 24-G catheter, 1.5–2.0 (maximum 2.5) ml/s for a 22-G catheter, 2–3 (maximum 4.0) ml/s for a 20-G catheter, and 3–3.5 (maximum 5.0) for a 16–18-G catheter |